A Chance-constrained Two-stage Stochastic Program for Unit Commitment with Uncertain Wind Power Output

Qianfan Wang, *Student Member, IEEE,* Yongpei Guan, *Member, IEEE,* Jianhui Wang, *Member, IEEE*

***Abstract*—In this paper, we present a unit commitment problem with uncertain wind power output. The problem is formulated as a chance-constrained two-stage (CCTS) stochastic program. Our model ensures that, with high probability, a large portion of the wind power output at each operating hour will be utilized. The proposed model includes both the two-stage stochastic program and the chance-constrained stochastic program features. These types of problems are challenging and have never been studied together before, even though the algorithms for the two-stage stochastic program and the chance-constrained stochastic program have been recently developed separately. In this paper, a combined sample average approximation (SAA) algorithm is developed to solve the model effectively. The convergence property and the solution validation process of our proposed combined SAA algorithm is discussed and presented in the paper. Finally, computational results indicate that increasing the utilization of wind power output might increase the total power generation cost, and our experiments also verify that the proposed algorithm can solve large-scale power grid optimization problems.**

***Index Terms*—Unit Commitment, Wind Power, Chance-constrained Optimization, Sample Average Approximation.**

NOMENCLATURE

A. Sets and Indices

BG	Set of buses with thermal generation units.
BW	Set of buses with wind farms.
B	Set of all buses.
$\mathcal{E}$	Set of transmission lines linking bus pairs.
Λ_b	Set of generators at bus b.
T	Time horizon (e.g., 24 hours).

B. Parameters

$k_{i,j}^b$	Line flow distribution factor for transmission line linking bus i and bus j due to the net injection at bus b.
$U_{i,j}$	Transmission flow limit on transmission line which links bus i and bus j.
D_{bt}	Demand at bus b in time period t.
μ_i^b	Start-up cost for generator i at bus b.
θ_i^b	Shut-down cost for generator i at bus b.
α_i^b	Cost of generating minimum power output for generator i if it is turned on at bus b.
$F_c(q_{it}^b)$	Fuel cost for generator i at bus b in time period t when its generation is q_{it}^b.
γ_t	Penalty cost per unit of energy shortage in time period t.
G_i^b	Minimum-up time for generator i at bus b.
H_i^b	Minimum-down time for generator i at bus b.
R_t	Amount of spinning reserve needed for the whole power system in time period t.
UR_i^b	Ramp-up rate limit of generator i at bus b.
DR_i^b	Ramp-down rate limit of generator i at bus b.
LB_i^b	Lower bound of electricity generated by generator i at bus b.
UB_i^b	Upper bound of electricity generated by generator i at bus b.
$w_{bt}(\xi)$	A random parameter indicating the wind power output or "available capacity" at bus b in time period t.

C. Decision Variables

Q_t^G	Total amount of electricity generated by thermal units in time period t.
Q_t^W	Total amount of wind power committed to be utilized (delivered) in time period t.
$\hat{q}_t^b$	Amount of wind power committed to be utilized (delivered) at bus b in time period t.
q_{it}^b	Amount of electricity generated by generator i at bus b in time period t.
o_{it}^b	Binary variable to indicate if generator i at bus b is on in time period t.
u_{it}^b	Binary variable to indicate if generator i at bus b is started up in time period t.
v_{it}^b	Binary variable to indicate if generator i at bus b is shut down in time period t.
$S_t^b(\xi)$	Amount of energy shortage at bus b in time period t (second-stage decision variable).

Qianfan Wang is with the Department of Industrial and Systems Engineering, University of Florida, Gainesville, FL 32611. E-mail: qfwang@ufl.edu.

Yongpei Guan is with the Department of Industrial and Systems Engineering, University of Florida, Gainesville, FL 32611. E-mail: guan@ise.ufl.edu.

Jianhui Wang is with the Argonne National Laboratory, Argonne, IL 60439. E-mail: jianhui.wang@anl.gov.

I. INTRODUCTION

High penetration of wind power has greatly challenged the way the power system has been operated. On one hand, wind power is sustainable and has zero carbon emissions. On the other hand, wind power is intermittent and very difficult to predict. The fluctuation in wind power output requires sufficient ramping capability available in the system to address the inherent variability and uncertainty. The traditional power system operation methods, which were designed to address

limited uncertainty in the system such as load variation, have failed to consider the variation from the unprecedented scale of wind power utilization. Hence, large-scale use of wind power production calls for advanced power system operation methods to maintain the security of system operations by better scheduling generation sources.

Research has been done to improve power system operation methods such as unit commitment (UC) to accommodate large amounts of wind power. A short-term generation scheduling model for Wind Power Integration in the Liberalised Electricity Markets (WILMAR) was proposed in [1], [2], and [3]. WILMAR is a stochastic rolling unit commitment model with wind power scenarios. The model has been successfully used in several wind integration studies. Ummels et al. [4] analyzed the impacts of wind power on thermal generation unit commitment and dispatch in the Dutch system, which has a significant share of combined heat and power (CHP) units. Bouffard and Galiana [5] used a stochastic unit commitment model to calculate the reserve requirements by simulating the wind power realization in the scenarios in comparison with the traditional pre-defined reserve requirements. Ruiz et al. [6] proposed a stochastic formulation to manage uncertainty in the unit commitment problem and extended the model to consider uncertainty and variability in wind power by using the same stochastic framework [7]. Wang et al. [8] presented a security-constrained unit commitment (SCUC) algorithm that takes into account the intermittency and variability of wind power generation. Benders' decomposition was used to decrease the computational requirements brought by a large number of wind power scenarios. A stochastic unit commitment model was proposed in [9]. Various wind power forecasts and different levels of reserve requirements were simulated. It was found that wind power forecast errors have significant impact on unit commitment and dispatch.

Most of the models presented so far aim to minimize the overall operating cost, which allows the curtailment of wind power. The wind power curtailment occurs when transmission congestion exists or there is oversupply of wind power due to the technical constraints of the other conventional units such as capacity or minimum on/off time constraints. In this case, the unused wind power becomes a waste. The wind power curtailment will dampen the incentive of wind power investment in the long run and may cause more emissions from the alternative energy sources. For these reasons, it is desirable that the system operators are able to utilize as much wind power as possible. In practice, the system operators in some regions like Germany are required to use renewable energy such as wind power as a priority over the other conventional generation sources [10]. Hence, because of the wind power uncertainty and variability, the system operators have reliability concerns in dispatching their systems with large amounts of wind power while wanting to utilize wind to the largest possible extent at the same time. Therefore, the system operators need to determine a proper unit commitment strategy which can balance the need to spill wind power due to reliability and other reasons while still taking the most advantage of wind power.

In this paper, we present a novel unit commitment model that can take into account wind power forecasting errors while maintaining the system reliability in case of sudden fluctuations in wind power output. In our model, the system operators can request a portion of the wind power output to be utilized at a certain probability. In this way, the risk of a large amount of wind being curtailed will be adjustable by the operators. We use the chance-constrained optimization technique to formulate the problem to ensure that, with high probability, a large portion of the wind power output at each operating hour will be utilized. Since the wind power uncertainty is captured by a number of wind power scenarios in our approach, a large part of the wind power output, defined by the system operators, will be utilized in a large portion of scenarios. The system operators can refine the unit commitment solution by defining appropriate attitudes toward risk and cost [11]. Some system operators may prefer a lower risk of curtailing the wind power while the others may be prone to spill wind power when system constraints take effect. The risk preference reflects the various treatments of wind power in reality [12].

Chance-constrained optimization has been previously studied to solve the stochastic unit commitment problem with uncertain load in [13] and transmission planning problem in [14]. In [13], with the consideration of the hourly load uncertainty and its correlation structure, the unit commitment problem is initially formulated as a chance constrained optimization problem in which the load is required to be met with a specified high probability over the entire time horizon. In the solution approach, the probability constraint is replaced by a set of separate probability constraints each of which could be inverted to obtain a set of equivalent deterministic linear inequalities. Finally, the deterministic form of the stochastic constraint is used in solving the problem iteratively. In [14], the chance constraint is applied to transmission planning, and it is in the form that the not-overload-probability for the transmission line is required to be more than a specified probability. Two-step optimization process with a genetic algorithm is applied to solve the problem.

In this paper, the chance constraint is applied to describe policies to ensure the utilization of wind power output. In our approach, different policies lead to different types of chance constraints. Some of these types of constraints could not be inverted to obtain equivalent deterministic linear inequalities. Thus, the algorithm developed in [13] could not be directly applied here to solve our problem. In addition, the algorithm proposed in [14] was not designed to solve two stage stochastic programs, and it also could not be directly applied here to solve our problem. Therefore, we propose to study a sample average approximation (SAA) algorithm to solve the problem. Our approach can provide a solution that converges to the optimal one as the number of samples increases.

The remaining part of this paper is organized as follows: Section II describes the background of chance-constrained and two-stage stochastic programming formulations, and provides the problem formulation. Section III presents the SAA solution framework, and shows the convergence property and related solution validation process of the SAA algorithm. Section IV describes the method to solve each sample in the SAA

algorithm. Numerical examples are provided in Section V. Section VI concludes the discussion.

II. Mathematical Formulation

A. Problem Formulation

Our model contains both chance-constrained and two-stage stochastic program features. We first briefly describe these two general models. The general chance-constrained stochastic problem can be described as follows:

$$\min_{x\in X} \ f(x) \ s.t. \ Pr\{G(x,\xi)\le 0\} \ge 1-\epsilon, \tag{1}$$

where $X \subset \Re^n$ denotes the deterministic feasible region, $f(x)$ represents the objective value to be minimized, ξ is a random vector whose probability distribution is supported on set $\Xi \subset \Re^d$, $G : \Re^n \times \Re^d \to \Re^m$ is a constraint mapping, 0 is an m dimensional vector of zeros, and $\epsilon \in (0,1)$ is given and usually called the risk level of the chance-constrained optimization. This formulation will minimize the objective function over a deterministic feasible set while $G(x,\xi) \le 0$ should be satisfied with a probability of at least $1-\epsilon$. It is intractable to solve a general chance-constrained stochastic problem because of the multidimensional chance constraint function and the non-convexity of the feasible region [15], [16].

The two-stage stochastic program [17] is another approach to address uncertainty, and the general formulation of the two-stage stochastic program with fixed recourse is shown as follows:

$$\min \ c^T x + E[Q(x,\xi)] \ s.t. \ Ax = b, x \ge 0, \tag{2}$$

where

$$Q(x,\xi) = \min \ \{qy(\xi) | Wy(\xi) = h - Tx, y(\xi) \ge 0\}. \tag{3}$$

Here, x denotes the first stage decision variable, $y(\xi)$ denotes the second-stage decision variable, and ξ is a random vector. This formulation minimizes the objective function which contains the expected value of recourse cost on second-stage variables.

In this paper, we develop a chance-constrained two-stage stochastic unit commitment formulation, combining (1), (2), and (3), to address uncertain wind power output. We call it a CCTS program, which contains both chance-constrained and two-stage stochastic program features. In our model, the only uncertainty considered is the wind power availability. The first stage of the stochastic program consists of the traditional unit commitment problem with transmission constraints and the decision on the total amount of wind power committed to be utilized (delivered), formed in light of a probabilistic wind power forecast. The second stage represents the penalty cost due to energy shortage once the actual wind power output is known. The chance constraint ensures the utilization of wind power output. The detailed formulation is described as follows (denoted as the true problem).

$$\min \sum_{b\in BG}\sum_{t=1}^{T}\sum_{i\in\Lambda_b}(\mu_i^b u_{it}^b + \theta_i^b v_{it}^b + \alpha_i^b o_{it}^b + F_c(q_{it}^b)) + \sum_{t=1}^{T}\gamma_t E\left[\sum_{b\in BW} S_t^b(\xi)\right] \tag{4}$$

$$s.t. \quad LB_i^b o_{it}^b \le q_{it}^b \le UB_i^b o_{it}^b \tag{5}$$
$$(\forall i\in\Lambda_b, \forall b\in BG, t=1,2,\ldots,T)$$
$$-o_{i(t-1)}^b + o_{it}^b - o_{ik}^b \le 0 \tag{6}$$
$$(1\le k-(t-1)\le G_i^b, \forall i\in\Lambda_b, \forall b\in BG, 1\le t\le T)$$
$$o_{i(t-1)}^b - o_{it}^b + o_{ik}^b \le 1 \tag{7}$$
$$(1\le k-(t-1)\le H_i^b, \forall i\in\Lambda_b, \forall b\in BG, 1\le t\le T)$$
$$-o_{i(t-1)}^b + o_{it}^b - u_{it}^b \le 0 \tag{8}$$
$$(\forall i\in\Lambda_b, \forall b\in BG, t=1,2,\ldots,T)$$
$$o_{i(t-1)}^b - o_{it}^b - v_{it}^b \le 0 \tag{9}$$
$$(\forall i\in\Lambda_b, \forall b\in BG, t=1,2,\ldots,T)$$
$$q_{it}^b - q_{i(t-1)}^b \le (2-o_{i(t-1)}^b - o_{it}^b)LB_i^b + (1+o_{i(t-1)}^b - o_{it}^b)UR_i^b \tag{10}$$
$$(\forall i\in\Lambda_b, \forall b\in BG, t=1,2,\ldots,T)$$
$$q_{i(t-1)}^b - q_{it}^b \le (2-o_{i(t-1)}^b - o_{it}^b)LB_i^b + (1-o_{i(t-1)}^b + o_{it}^b)DR_i^b \tag{11}$$
$$(\forall i\in\Lambda_b, \forall b\in BG, t=1,2,\ldots,T)$$
$$Q_t^G + Q_t^W = \sum_{b\in B} D_{bt} \tag{12}$$
$$(t=1,2,\ldots,T)$$
$$\sum_{b\in BW} \hat{q}_t^b = Q_t^W \tag{13}$$
$$(t=1,2,\ldots,T)$$
$$\sum_{b\in BG}\sum_{i\in\Lambda_b} q_{it}^b = Q_t^G \tag{14}$$
$$(t=1,2,\ldots,T)$$
$$\sum_{b\in BG}\sum_{i\in\Lambda_b} UB_i^b o_{it}^b \ge R_t + \sum_{b\in B} D_{bt} \tag{15}$$
$$(t=1,2,\ldots,T)$$
$$-U_{ij} \le \sum_{b\in B} k_{ij}^b(\hat{q}_t^b + \sum_{n\in\Lambda_b} q_{nt}^b - D_{bt}) \le U_{ij} \tag{16}$$
$$(\forall (i,j)\in\mathcal{E}, t=1,2,\ldots,T)$$
$$Pr(G(x,\xi)\le 0) \ge 1-\epsilon \tag{17}$$
$$S_t^b(\xi) = \max\{0, \hat{q}_t^b - w_{bt}(\xi)\} \tag{18}$$
$$(\forall b\in BW; t=1,2,\ldots,T; \xi\in\Xi\subset\Re^{|B|\times T}).$$
$$q_{it}^b, \hat{q}_t^b \ge 0; o_{it}^b, u_{it}^b, v_{it}^b \in \{0,1\}, \forall t, \forall i, \forall b. \tag{19}$$

In the above formulation, the decision variables $S_t^b(\xi)$ are second-stage variables, corresponding to y in (1)–(3), and others are first stage variables, corresponding to x in (1)–(3). We define $F_c(q_{it}^b) = c_i^b(q_{it}^b)^2 + b_i^b q_{it}^b$. Note here because of constraints (5), we have $\alpha_i^b o_{it}^b + F_c(q_{it}^b) = (c_i^b(q_{it}^b)^2 + b_i^b q_{it}^b + \alpha_i^b)o_{it}^b$. The objective function (4) is composed of power generation costs in the first stage and penalty cost due to energy shortage in the second stage. In our model, for each time period in the second stage, if the wind power output is

larger than the amount of wind power committed to be utilized, the excess wind power can be curtailed without penalty, because the utilization of wind power usage is guaranteed by the chance constraint (17). Excess wind power will not be sold to a third party with the consideration of potential transmission congestion and other constraints. If the wind power output is less than the amount of wind power committed to be utilized, penalty cost will be triggered due to energy shortage. The hourly UC constraints listed above include the unit generation capacity constraints (5), unit minimum-up time constraints (6) (e.g., when $o^b_{i(t-1)} = 0$ and $o^b_{it} = 1$, it means that the unit is turned on in time period t. Then in the following G^b_i time periods, it should be on, because we have $-0 + 1 - o^b_{ik} \leq 0$ at this moment, and $o^b_{ik} = 1$ can be guaranteed for at least G^b_i time periods), unit minimum-down time constraints (7) (the explanation is similar to the one for (6)), unit start-up constraints (8), unit shut-down constraints (9), unit ramping up constraints (10), unit ramping down constraints (11), system power balance constraints (12, 13, 14), system spinning reserve requirements (15), and transmission capacity constraints (16) (Note that the calculation of k^b_{ij} is the same as the one described in [18]). Constraints (5)-(16) are first stage constraints; constraint (17) indicates that $G(x, \xi) \leq 0$ (for notation brevity, we use x to represent all the first stage decision variables) should be satisfied with a probability of at least $1-\epsilon$; constraint (17) is described in detail in the following part B; constraints (18) are the second-stage constraints which indicate the amount of energy shortage, in case the wind power output is less than the amount of wind power committed to be utilized.

B. Chance Constraint Description

We apply three policies to guarantee the utilization of wind power and develop the corresponding three types of chance constraints with constraint mappings G^1, G^2 and G^3, respectively.

1) Policy 1: Constraint mapping G^1 defines that for the entire time planning horizon (24h), there is at least $1-\epsilon$ chance the usage of the total wind power generation is larger than or equal to $\beta,\ 0 < \beta < 100\%$.

$$Pr(\beta \sum_{t=1}^{T} \sum_{b \in BW} w_{bt}(\xi) - \sum_{t=1}^{T} Q^W_t \leq 0) \geq 1 - \epsilon. \qquad (20)$$

2) Policy 2: Constraint mapping G^2 defines that for each particular operating hour on the time planning horizon, there is at least $1 - \epsilon$ chance the usage of the wind power is larger than or equal to $\beta,\ 0 < \beta < 100\%$.

$$Pr(\beta \sum_{b \in BW} w_{bt}(\xi) - Q^W_t \leq 0) \geq 1 - \epsilon, \qquad (21)$$
$$(t = 1, 2, \ldots, T).$$

3) Policy 3: Constraint mapping G^3 considers the joint probability which is at least $1 - \epsilon$ chance the usage of wind power is larger than or equal to $\beta,\ 0 < \beta < 100\%$ for every operating hour.

$$Pr(\beta \sum_{b \in BW} w_b(\xi) - Q^W \leq 0) \geq 1 - \epsilon, \qquad (22)$$

where $w_b(\xi) = [w_{b1}(\xi), w_{b2}(\xi), \ldots, w_{bT}(\xi)]^T$, $Q^W = [Q^W_1, Q^W_2, \ldots, Q^W_T]^T$, and 0 is a T dimensional vector of zeros.

From above, it can be observed that policy 3 is most restrictive, while policy 1 is the least restrictive one. In policy 3, we require that at least β of wind power is utilized during each of the 24 operating hours to make an outcome of the random wind generation amount a qualified one (i.e., satisfying the chance constraint). Thus, policy 3 is more restrictive than policy 2, which is more restrictive than policy 1.

III. Sample Average Approximation

Sample average approximation (SAA) is an effective method to solve chance-constrained and two-stage stochastic problems. The basic idea of SAA is to approximate the true distribution of random variables with an empirical distribution by Monte Carlo sampling technology. A number of theoretical research and computational studies of SAA have been developed for chance-constrained stochastic problems (e.g., [16] and [19]) and two-stage stochastic problems (e.g., [20] and [21]). However, there is no existing SAA method to solve the model that contains both chance-constrained and two-stage stochastic program features. In this section, we develop a combined SAA algorithm to solve the CCTS program. The combined SAA framework contains three parts: scenario generation, convergence analysis, and solution validation. For each SAA problem, we solve the corresponding mixed-integer-linear program (MILP) efficiently by developing a strong formulation. The details are shown in the following subsections.

A. Scenario Generation

In SAA, the true distribution of wind power generation is replaced by an empirical distribution using computer simulation. We use Monte Carlo simulation to generate scenarios. Assume the wind power is subject to a multivariate normal distribution $N(\mu, \Sigma)$ (one of many possible distributions of wind power) for every time period t, where vector μ is chosen as the forecasted wind power and matrix Σ describes the volatility. The Monte Carlo simulation generates a large number of scenarios, each with the same probability $1/N$. In each scenario, there are 24 hourly, random wind power outputs based on the forecasted generation. To decrease the variance of simple Monte Carlo simulation, the Latin hypercube sampling (LHS) is employed to make the statistical distribution fit the real distribution better [8].

After the scenarios are generated (e.g., N scenarios), the expected value function $E[\sum_{b \in BW} S^b_t(\xi)]$ is estimated by the sample average function $N^{-1} \sum_{j=1}^{N} \sum_{b \in BW} S^b_t(\xi^j)$ (see, e.g., [20]). On the other hand, in general, the chance constraint can be estimated by an indicator function $N^{-1} \sum_{j=1}^{N} \mathbb{1}_{(0,\infty)}(G(x, \xi^j)) \leq \epsilon$ (see, e.g., [16]), which requires that a certain percentage of the samples satisfy the chance constraint. The value of the indicator function $\mathbb{1}_{(0,\infty)}(G(x, \xi^j))$ is equal to one when $G(x, \xi^j) \in (0, \infty)$ or zero when $G(x, \xi^j) \leq 0$. The corresponding formulation is

shown as follows (denoted as the SAA problem):

$$\begin{aligned}
&\min \sum_{b\in BG}\sum_{t=1}^{T}\sum_{i\in\Lambda_b}(\mu_i^b u_{it}^b+\theta_i^b v_{it}^b+\alpha_i^b o_{it}^b+F_c(q_{it}^b))\\
&+N^{-1}\sum_{t=1}^{T}\sum_{j=1}^{N}\gamma_t\sum_{b\in BW}S_t^b(\xi^j)\\
&s.t.(5)-(16)\\
&N^{-1}\sum_{j=1}^{N}\mathbb{1}_{(0,\infty)}(G(x,\xi^j))\le\epsilon\\
&\hat{q}_t^b\le w_{bt}(\xi^j)+S_t^b(\xi^j)\\
&\quad(\forall t;\forall b\in BW;j=1,2,\ldots,N)\\
&q_{it}^b,\hat{q}_t^b,S_t^b(\xi^j)\ge 0;o_{it}^b,u_{it}^b,v_{it}^b\in\{0,1\},\forall t,\forall i,\forall b.
\end{aligned}$$

First, as the sample size N goes to infinity, we can prove that the objective of the above formulation converges to that of the true problem as shown in the following proposition.

Proposition 1: Let $\hat{\theta}_N$ represent the objective value of the SAA problem, and θ^* represent the objective value of the true program. We have $\hat{\theta}_N\to\theta^*$ and $D(\hat{x}_N,x^*)\to 0$ w.p.1 as $N\to\infty$, where $D(\hat{x}_N,x^*)$ represents the distance between the optimal solution $\hat{x}_N$ for the SAA problem and the optimal solution x^* for the true problem.

Proof: The details of the convergence proof are given in Appendix A. ∎

Next, we discuss the solution validation process in the following subsection.

B. Solution Validation

Solution validation for the two-stage and chance-constrained problems have been well studied in [16] and [21], respectively. In this section, we develop a combined algorithm that embeds the solution validation of the chance-constrained problem into that of the two-stage problem.

Assume that $\bar{x}$ is an optimal solution for the SAA problem, and $\bar{v}$ is the corresponding objective value. For a given candidate solution for the SAA problem, solution validation provides a scheme to validate its quality by obtaining upper and lower bounds for the corresponding optimal objective value. We construct the upper and lower bounds as follows:

1) Upper Bound: Since CCTS contains a chance constraint, we start with the verification of feasibility of the given solution $\bar{x}$. To do this, we first estimate the true probability function of the chance constraint

$$q(\bar{x})=Pr\{G(\bar{x},\xi)>0\}. \tag{23}$$

Following the method described in [15] and [16], we construct a $(1-\tau)$-confidence upper bound on $q(\bar{x})$:

$$U(\bar{x})=\hat{q}_{N'}(\bar{x})+z_\tau\sqrt{\hat{q}_{N'}(\bar{x})(1-\hat{q}_{N'}(\bar{x}))/N'}, \tag{24}$$

where N' is the sample size for the validation of the chance constraint, and $\hat{q}_{N'}(\bar{x})$ is the estimated value of $q(\bar{x})$ for the given sample size N'.

If this upper bound of $q(\bar{x})$ is less than the risk level ϵ, then $\bar{x}$ is feasible with confidence level $(1-\tau)$. Then, we can evaluate the corresponding upper bound of the optimal value for the second-stage part in CCTS, the same as the validation process for the normal two-stage stochastic problem as described in [21]:

$$U(\bar{v})=c^T\bar{x}+\frac{1}{N'}\sum_{n=1}^{N'}Q(x,\xi^n). \tag{25}$$

It is easy to see that $U(\bar{v})$ is the upper bound for CCTS.

2) Lower bound: To get the lower bound for the objective value $\bar{v}$, we take $\hat{S}$ iterations. For each iteration $1\le s\le\hat{S}$, we run the N scenario SAA problem M times. For these M runs, we follow the same scheme as the one described in [15] and [16] to pick the Lth smallest optimal value, denoted as $\bar{v}_{L_s}$, as the approximated lower bound for the chance-constrained part with confidence level $(1-\tau)$, where L is calculated as described in [16]. Finally, taking the average of $\{\bar{v}_{L_s},1\le s\le\hat{S}\}$ provides the lower bound for CCTS.

C. Summary of the Combined SAA Algorithm

In the algorithm, we put the calculation of the upper bound for CCTS in the loop of the calculation of the lower bound for the chance-constrained part in order to speed up the algorithm. The proposed combined SAA algorithm is summarized in the following steps (also see flowchart in Fig. 1).

1. For $s=1,2,\ldots,\hat{S}$, repeat the following steps:
   (1) For $m=1,2,\ldots,M$, repeat the following steps:
   (a) Solve the associated SAA with N scenarios. Denote the solution as $\bar{x}_m$ and the optimal value as $\bar{v}_m$;
   (b) Generate scenarios $\xi^1,\xi^2,\ldots,\xi^{N'}$. Estimate $q(\bar{x}_m)$ by $\hat{q}_{N'}(\bar{x}_m)$ and use (24) to get $U(\bar{x}_m)$;
   (c) If $U(\bar{x}_m)\le\epsilon$, go to (d); else, skip (d) and go to next iteration;
   (d) Estimate the corresponding upper bound for CCTS using (25), based on the N' scenarios generated in (b);
   (2) Pick the smallest upper bound in Step (1) as the approximated upper bound $\hat{g}^s$;
   (3) Sort the M optimal values obtained in Step (1) in nondecreasing order, e.g., $\bar{v}_1\le\bar{v}_2\le\ldots\bar{v}_M$. Pick the Lth optimal value $\bar{v}_L$ and denote it as $\bar{v}_{L_s}$.

2. Taking the average of $\bar{v}_{L_1},\bar{v}_{L_2},\ldots,\bar{v}_{L_{\hat{S}}}$, we get the lower bound $\bar{v}=\frac{1}{\hat{S}}\sum_{s=1}^{\hat{S}}\bar{v}_{L_s}$.

3. Taking the minimum of $\hat{g}^1,\hat{g}^2,\ldots,\hat{g}^{\hat{S}}$, we get the upper bound $\hat{g}=\min_{1\le s\le\hat{S}}\hat{g}^s$.

4. Estimate the optimality gap given by $(\hat{g}-\bar{v})/\bar{v}\times 100\%$.

IV. Methods To Solve The SAA Problem

The SAA problem is an MILP. We can use the standard branch and bound algorithm which is implemented in most commercial solvers. The main problem is how to solve the SAA problem effectively with the chance constraints under different policies. In this section, we introduce a sorting approach for policies 1 and 2. For policy 3, we derive a strong formulation as studied in [19] to speed up the algorithm.

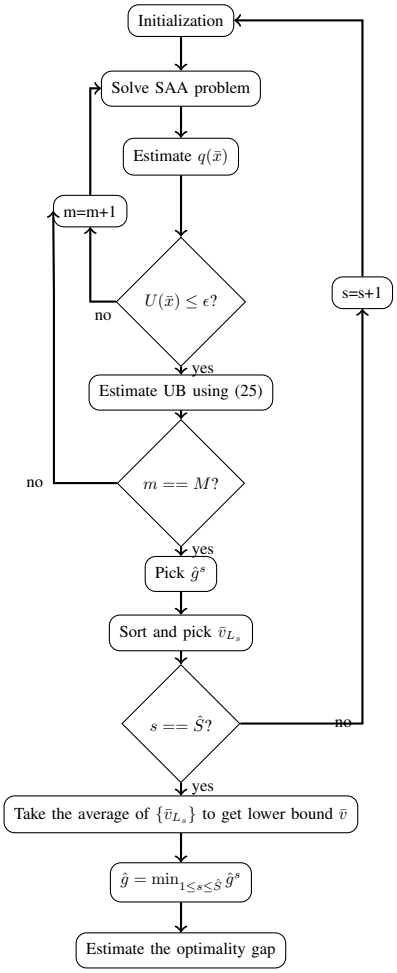

Fig. 1. Proposed Combined SAA Algorithm

A. Sorting Approach

After taking samples, we can simplify (20) by sorting the right-hand-side values of the constraints for each sample, (i.e., wind power in each day) and picking the $\lceil (1-\epsilon) \times N \rceil$th right-hand-side value to construct a deterministic constraint. Similarly, after taking samples, we can simplify (21) by sorting the right-hand-side values of the constraints for each sample (i.e., wind power in each hour) and picking the $\lceil (1-\epsilon) \times N \rceil$th right-hand-side value to construct a deterministic constraint.

B. Strong Formulation

It can be observed that the sorting method does not work for (22) because the sorting algorithm cannot handle the joint probability case described in (22). Instead, reformulating as an MILP allows solution of the problem incorporating (22). For a given sample size N, constraint (22) can be reformulated as follows:

$$\begin{aligned}
&\beta \sum_{b \in BW} w_{bt}(\xi^j) - Q_t^W \leq M \times z_j \\
&\qquad (t = 1, 2, \ldots, T; j = 1, 2, \ldots, N) \\
&\sum_{j=1}^{N} z_j \leq N \times \epsilon \\
&z_j \in \{0, 1\} \\
&\qquad (j = 1, 2, \ldots, N).
\end{aligned}$$

The star-inequalities can speed up the computation of the above MILP model (see, e.g., [16], [19], and [22]). Moreover, it has been proved that the MILP model can be transformed into a strong formulation after adding the star-inequalities [19]. To do this, we introduce a new set of binary variables $\{r_{tj} : j = 1, 2, \ldots, q; t = 1, 2, \ldots, T\}$ and define $h_{tj} = \beta \sum_{b \in BW} w_{bt}(\xi^j)$. Without loss of generality, we assume that $h_{t1} \geq h_{t2} \geq \cdots \geq h_{tN}$. The strong formulation is described as follows:

$$\begin{aligned}
&r_{tj} - r_{t(j+1)} \geq 0 \\
&\qquad (j = 1, 2, \ldots, q; t = 1, 2, \ldots, T) \\
&z_{[j]} - r_{tj} \geq 0 \\
&\qquad (j = 1, 2, \ldots, q; t = 1, 2, \ldots, T) \\
&Q_t^W + \sum_{j=1}^{q} (h_{tj} - h_{t(j+1)}) r_{tj} \geq h_{t1} \qquad (26) \\
&\qquad (t = 1, 2, \ldots, T) \\
&\sum_{j=1}^{N} z_j \leq N \times \epsilon \\
&r_{tj}, z_j \in \{0, 1\},
\end{aligned}$$

where $[j]$ represents the scenario index corresponding to the jth largest h value in time period t, and inequalities (26) are the star inequalities.

V. Computational Result

In this section, a six-bus system and a revised 118-bus system are studied to illustrate the proposed algorithms. In the six-bus system, we run the computational experiments at different risk levels to compare the results of different policies. The solution validation is neglected for simplicity, and computational experiments at different sample sizes are tested to verify the convergence property of the combined SAA algorithm. In the revised 118-bus system, we run the computational experiments to test the entire combined SAA algorithm described in Sections III and IV. The algorithm is coded in C++ using CPLEX 12.1. All experiments are implemented on a computer workstation with Intel Quad Core 2.40GHz and 8GB memory.

A. Six-bus System

The six-bus system includes three generators, one wind farm, three loads, and six transmission lines. The layout of the system is depicted in Fig. 2, and the characteristics of the buses, thermal units, and transmission lines are described in Tables I-IV.

We assume the wind farm is located at bus B_4, $\beta = 85\%$, and $\gamma_t = 600, \ \forall t$. The wind power is assumed multivariate normal distributed, with the hourly mean forecasted outputs ranging between $10 - 100$ and a standard deviation of 45% of the expected values. To run the model in CPLEX effectively, we use the interpolation method [23] to approximate the fuel cost function. A piecewise linear function replaces the fuel cost function in (4).

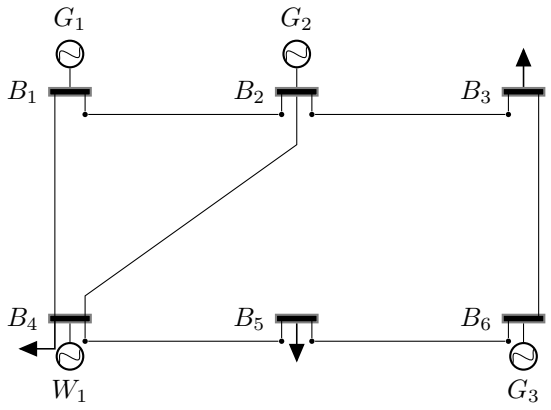

Fig. 2. Six-bus System

TABLE I
BUS DATA

Bus ID	Type	Unit	Wind Farm	Hourly Load (MW)
B_1	Thermal	G_1	-	-
B_2	Thermal	G_2	-	-
B_3	Thermal	-	-	300
B_4	Wind	-	W_1	300
B_5	Thermal	-	-	200
B_6	Thermal	G_3	-	-

TABLE II
GENERATOR DATA

Unit	Lower (MW)	Upper (MW)	Min-down (h)	Min-up (h)	Ramp (MW/h)
G_1	100	300	2	4	50
G_2	80	200	3	3	40
G_3	150	350	3	2	15

TABLE III
FUEL DATA

Unit	α (MBtu)	b (MBtu/MWh)	c (MBtu/MW^{2}h)	Start-up Fuel (MBtu)	Fuel Price ($/MBtu)
G_1	50	6	0.0004	100	1.2469
G_2	40	5.5	0.0001	300	1.2461
G_3	60	4.5	0.005	0	1.2462

TABLE IV
TRANSMISSION LINE DATA

Line ID	From	To	X	Flow Limit (MW)
L_1	B_1	B_2	0.170	200
L_2	B_1	B_4	0.150	200
L_3	B_2	B_3	0.258	300
L_4	B_2	B_4	0.197	200
L_5	B_3	B_6	0.140	100
L_6	B_4	B_5	0.150	200
L_7	B_5	B_6	0.160	400

1) A 5-scenario Example: We first give an example with 5 scenarios to illustrate Policy 3. Based on the chance constraint description in Policy 3 with $\epsilon = 20\%$, there is only one scenario in which there are time periods whose wind utilizations are less than 85%. From the results shown in Figure 3, we can

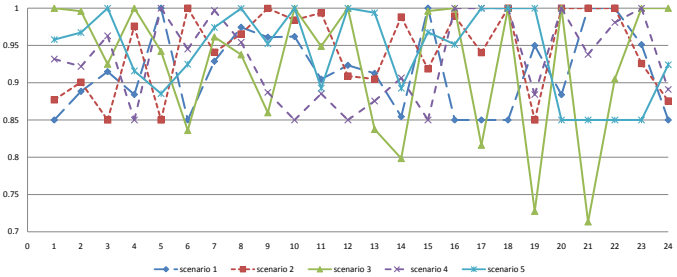

Fig. 3. Wind Utilization in Each Operating Hour for the 5 Scenario Case

observe that the chance constraint is satisfied and only scenario 3 can have utilization below 85%. The unit commitment results in the optimal solution are listed in Table V.

TABLE V
OPTIMAL UNIT COMMITMENT

T	Hours (1-24)
G_1	1 1 1 1 1 1 1 1 1 1 1 1 1 1 1 1 1 1 1 1 1 1 1 1
G_2	0 0 0 0 0 0 0 1 1 1 1 1 1 1 1 1 1 1 1 1 1 1 1 1
G_3	1 1 1 1 0 0 0 1 1 1 1 1 1 1 1 1 0 0 0 0 0 0 0 0

2) Experiments at Different Risk Levels: Next, we use 200 scenarios to run experiments on different risk levels. The results are reported in Tables VI, VII, and VIII for comparison.

It can be observed that the total cost (column "obj." in Table VIII) is reduced as the risk level increases from 15% to 100%. This is reasonable because the fuel cost for thermal plants might be higher if the policy on wind power generation is more restrictive and less wind power will be curtailed. An extreme case is $\epsilon = 100\%$ in which the chance constraint can be neglected. In such a case, the optimal cost is smaller than that at any other risk level. Meanwhile, the wind utilization is at its lowest value as well (below 50%). Here the wind utilization is measured as the average wind usage under all scenarios, which is equal to the ratio between $\sum_{t=1}^{T}\sum_{j=1}^{200}\sum_{b\in BW}\min\{\hat{q}_t^b, w_{bt}(\xi^j)\}$ and $\sum_{t=1}^{T}\sum_{j=1}^{200}\sum_{b\in BW} w_{bt}(\xi^j)$. From Tables VI-VIII, we can also observe that Policy 3 is the most restrictive one. For the same given risk level, the wind power utilization is the highest among all three polices.

TABLE VI
COMPUTATIONAL RESULTS FOR THE SIX-BUS SYSTEM WITH DIFFERENT RISK LEVELS - USING POLICY 1

Risk Level ϵ	Obj. ($)	Utilization	CPU Time (sec)
15%	53038.3	84.01%	0.29
20%	52541.3	83.04%	0.31
40%	51473.3	81.92%	0.25
70%	48235.5	75.01%	0.29
100%	46213.8	48.9%	0.11

3) Experiments at Different Scenario Sizes: We have shown the convergence property of the combined SAA algorithm in Section III. Here, we set different sample sizes for the SAA

TABLE VII
COMPUTATIONAL RESULTS FOR THE SIX-BUS SYSTEM WITH DIFFERENT RISK LEVELS - USING POLICY 2

Risk Level ϵ	**Obj. ($)**	**Utilization**	**CPU Time (sec)**
15%	63315.5	90.00%	0.02
20%	60462.5	88.75%	0.07
40%	53782.1	83.57%	0.08
70%	48699.1	75.09%	0.1
100%	46213.8	48.9%	0.11

TABLE VIII
COMPUTATIONAL RESULTS FOR THE SIX-BUS SYSTEM WITH DIFFERENT RISK LEVELS - USING POLICY 3

Risk Level ϵ	**Obj. ($)**	**Utilization**	**CPU Time (sec)**
15%	79372.5	93.86%	1.47
20%	76850.5	93.5%	2.07
40%	69268.3	92.2%	3.85
70%	62789.5	90.14%	53.28
100%	46213.8	48.9%	0.11

algorithm to verify that the optimal solution indeed converges as the scenario size increases (e.g., see Fig. 4). Policy 3 is applied and the risk level is set to $\epsilon = 10\%$ for comparison.

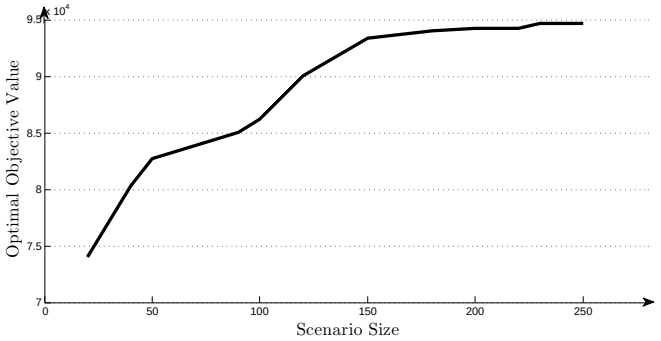

Fig. 4. Plotting the Solutions of SAA with Different Scenario Sizes

B. Modified 118-bus System

A modified IEEE 118-bus system, based on the one given online at motor.ece.iit.edu/data, is used to test the SAA algorithm. We select all the generators that use coal as the fuel. In total, there are 33 thermal generators. We take all 186 transmission lines and 91 loads. Since there are only 33 generators, we reduce the value of the load at each bus to ensure the existence of a solution. Additionally, we consider a wind farm at Bus 3, the risk level $\epsilon = 10\%$, and $\beta = 85\%$. The detailed revised 118-bus system data is given online at cso.ise.ufl.edu/data_r118.xls.

We then apply policy 3, and the computational results are reported in Table IX. The first column represents the combination of iteration numbers $(\hat{S}, M)$ (i.e., iteration numbers for obtaining the lower bound and for the chance constraint part), and validation's scenario size (N'). The second column represents the scenario size of the SAA problem. The third column represents the lower bound obtained by the SAA algorithm. The fourth column represents the upper bound obtained by the SAA algorithm. The fifth column represents the gap which is calculated by $\frac{UB-LB}{LB} \times 100\%$. Finally, the sixth column represents the CPU time of the algorithm.

TABLE IX
COMPUTATIONAL RESULTS FOR THE 118-BUS SYSTEM

$(\hat{S} \times M, N')$	N	LB	UB	Gap	Time (sec)
$(5 \times 5, 1000)$	10	470290	477184	1.46%	3.6
	50	472839	477210	0.9%	6.75
	100	473578	477857	0.9%	10.2
$(5 \times 20, 2000)$	10	471994	475233	0.6%	15.8
	50	474271	476325	0.4%	25.4
	100	474560	477562	0.6%	40.3
$(20 \times 20, 3000)$	10	472356	473995	0.34%	64.5
	50	474692	476230	0.32%	103.8
	100	474701	476125	0.30%	145.8

From Table IX, we can observe that as the iteration number and the sample size increase, the optimality gap decreases. For the last case in which the sample size is 100, the iteration numbers are $\hat{S} = M = 20$, and the validation scenario size $N' = 3000$, the optimality gap is around 0.30%. That is, the proposed algorithm converges fast and can solve the problem effectively.

Finally, we compare the performance between the default MILP and the strong formulation approaches, and report the results in Table X. It can be observed from the table that the strong formulation approach takes much less time than the default MILP approach when the risk level is not trivial (e.g., $0 < \epsilon < 100\%$). The results show the scalability of the strong formulation approach to solve large-scale problems. It can also be observed from the table that the optimal objective value decreases as the risk level increases.

TABLE X
COMPUTATIONAL TIME FOR THE 118-BUS SYSTEM: MILP AND STRONG FORMULATION

ϵ	N	Obj.($)	MILP (sec)	Strong (sec)
0%	100	477463	0.16	0.16
	150	481947	0.2	0.18
	200	482059	0.23	0.21
20%	100	472759	8.08	0.3
	150	472833	54.16	0.49
	200	473072	154.51	0.57
100%	100	468712	0.19	0.21
	150	468924	0.21	0.24
	200	468883	0.25	0.29

VI. CONCLUSION

In this paper, a chance constrained two-stage stochastic program considering the uncertain wind power output was studied. In our approach, the chance constraint guarantees the minimum usage of the wind power by setting a risk level, which limits the chance that a large amount of wind power might be curtailed. We studied three different types of polices and compared the wind utilizations by these policies. The results verified that Policy 3 is the most restrictive one. Then, we studied a combined SAA algorithm that can derive an optimal solution when the sample size increases. The final

computational results verify the effectiveness of the proposed SAA algorithm and the related solution validation process, and show that the proposed model can help increase the usage of wind power.

ACKNOWLEDGMENTS

The authors would like to thank the editor and the reviewers for their sincere suggestions on improving the quality of this paper. This research was partly supported by the U.S. National Science Foundation under CAREER Award CMMI-0748204 and by the U.S. Department of Defense under Office of Naval Research Young Investigator Award N000141010749.

APPENDIX A
PROOF OF PROPOSITION 1

Convergence proofs for the chance-constrained and the two-stage stochastic programs have been studied in [16] and [21], respectively. This paper, however, provides the first proof for the case that contains both chance-constrained and two-stage stochastic program features.

In our CCTS program, the samples of the random variable (wind generation) are used in the approximations for both the second-stage value and the chance constraint part. Once the samples are generated, the stochastic problem will become a deterministic problem. We show in this part that the objective of the deterministic problem is convergent to that of the stochastic problem as the scenario size goes to infinity.

Recall that our CCTS program (e.g., the true problem) can be expressed as follows:

$$\begin{aligned}
&\min \sum_{b\in BG}\sum_{t=1}^{T}\sum_{i\in\Lambda_b}(\mu_i^b u_{it}^b+\theta_i^b v_{it}^b+\alpha_i^b o_{it}^b+F_c(q_{it}^b))\\
&+\sum_{t=1}^{T}\gamma_t E[\sum_{b\in BW} S_t^b(\xi)] \qquad (27)\\
&s.t.\\
&(5)-(16)\\
&Pr\{G(x,\xi)\le 0\}\ge 1-\epsilon\\
&S_t^b(\xi)=\max\{0,\hat{q}_t^b-w_{bt}(\xi)\},\forall t,\forall\xi,\forall b\in BW\\
&q_{it}^b,\hat{q}_t^b\ge 0; o_{it}^b,u_{it}^b,v_{it}^b\in\{0,1\},\forall t,\forall i,\forall b.
\end{aligned}$$

Before starting the proof of the convergence, we introduce the following two approximated models:

(i) Replace the chance-constrained part by the sample approximation.

$$\begin{aligned}
&\min \sum_{b\in BG}\sum_{t=1}^{T}\sum_{i\in\Lambda_b}(\mu_i^b u_{it}^b+\theta_i^b v_{it}^b+\alpha_i^b o_{it}^b+F_c(q_{it}^b))\\
&+\sum_{t=1}^{T}\gamma_t E[\sum_{b\in BW} S_t^b(\xi)] \qquad (28)\\
&s.t.\\
&(5)-(16)\\
&N^{-1}\sum_{j=1}^{N}\mathbb{1}_{(0,\infty)}(G(x,\xi^j))\le\epsilon\\
&S_t^b(\xi)=\max\{0,\hat{q}_t^b-w_{bt}(\xi)\},\forall t,\forall\xi,\forall b\in BW\\
&q_{it}^b,\hat{q}_t^b\ge 0; o_{it}^b,u_{it}^b,v_{it}^b\in\{0,1\},\forall t,\forall i,\forall b.
\end{aligned}$$

(ii) Replace both the chance-constrained and the second-stage parts by the sample approximation.

$$\begin{aligned}
&\min \sum_{b\in BG}\sum_{t=1}^{T}\sum_{i\in\Lambda_b}(\mu_i^b u_{it}^b+\theta_i^b v_{it}^b+\alpha_i^b o_{it}^b+F_c(q_{it}^b))\\
&+N^{-1}\sum_{t=1}^{T}\sum_{j=1}^{N}\gamma_t\sum_{b\in BW} S_t^b(\xi^j) \qquad (29)\\
&s.t.\\
&(5)-(16)\\
&N^{-1}\sum_{j=1}^{N}\mathbb{1}_{(0,\infty)}(G(x,\xi^j))\le\epsilon\\
&\hat{q}_t^b\le w_{bt}(\xi^j)+S_t^b(\xi^j)\\
&\quad(\forall t;\forall b\in BW; j=1,2,\ldots,N)\\
&q_{it}^b,\hat{q}_t^b,S_t^b(\xi^j)\ge 0; o_{it}^b,u_{it}^b,v_{it}^b\in\{0,1\},\forall t,\forall i,\forall b.
\end{aligned}$$

Before we give the detailed proof of the proposition, we show a corollary based on an assumption and Proposition 2 in [16].

Assumption 1: There is an optimal solution $\bar{x}$ of the true problem (1) such that for any $\nu>0$ there is $x\in X$, where X is the feasible region for the problem, with $\|x-\bar{x}\|\le\nu$ and $q(x)\le\epsilon$.

Proposition 2: Suppose that the significance levels of the true and SAA problems are the same (i.e., $\epsilon=\epsilon_N$), the set X is compact, the function $f(x)$ and decision variables are continuous, $G(x,\xi)$ is a Caratheodory function, and the above assumption holds, then $\hat{\theta}_N\to\theta^*$ and $D(\hat{x}_N,x^*)\to 0$ $w.p.1$ as $N\to\infty$.

In Proposition 2, the convergence property holds for the continuous case. Now we show the convergence property holds for the mixed integer case in the following corollary.

Corollary 1: For the mix-integer case, suppose the objective function is $f(x,y)$, where $x\in X$ is the set of binary variables, and $y\in Y$ is the set of continuous variables. If X is finite, and the other assumptions in the above proposition hold, then, we still have $\hat{\theta}_N\to\theta^*$ and $D(\hat{x}_N,x^*)\to 0$ $w.p.1$ as $N\to\infty$.

Proof: Let $|X|=\Gamma$. We denote the elements of set X in order: $x^1,x^2,\ldots,x^\Gamma$. For each fixed x^i, we can apply Proposition 2 for continuous variable y and get a corresponding convergent solution by solving the SAA problem, i.e.,

$$\min\{f_N(x^j,y)\}\to\min\{f(x^j,y)\}\equiv g(x^j), \qquad (30)$$

where $f_N(.,.)$ represents the objective function for the SAA problem when the sample size is N.

Without loss of generality, we assume

$$\sigma=\min_{1\le i,j\le\Gamma}\parallel g(x^i)-g(x^j)\parallel>0. \qquad (31)$$

Now let x^* be the integer part in the optimal solution of the true problem, and $\hat{x}_N$ be the integer part in the optimal solution of the SAA problem when the sample size is N.

Based on (30), there exists a large constant number N_0 such that

$$\| f_N(\hat{x}_N, \hat{y}_N) - g(\hat{x}_N) \| < \frac{\sigma}{2} \tag{32}$$

and

$$\| f_N(x^*, \hat{y}_N) - g(x^*) \| < \frac{\sigma}{2}, \tag{33}$$

when $N > N_0$. Meanwhile, we should have

$$f_N(x^*, \hat{y}_N) \geq f_N(\hat{x}_N, \hat{y}_N), \tag{34}$$

since $(\hat{x}_N, \hat{y}_N)$ is the optimal solution for the SAA problem when the sample size is N.

On the other hand, it is obvious that

$$g(\hat{x}_N) \geq g(x^*), \tag{35}$$

based on the definition of x^*. If $\hat{x}_N \neq x^*$, then based on (34) and (35),

$$0 \leq g(\hat{x}_N) - g(x^*) \leq g(\hat{x}_N) - g(x^*) + f_N(x^*, \hat{y}_N) - f_N(\hat{x}_N, \hat{y}_N).$$

Thus

$$\begin{aligned} &\| g(\hat{x}_N) - g(x^*) \| \\ \leq &\| g(\hat{x}_N) - g(x^*) + f_N(x^*, \hat{y}_N) - f_N(\hat{x}_N, \hat{y}_N) \| \\ \leq &\| g(\hat{x}_N) - f_N(\hat{x}_N, \hat{y}_N) \| + \| g(x^*) - f_N(x^*, \hat{y}_N) \| \\ < &\sigma, \end{aligned}$$

where the third inequality follows from (32) and (33). This contradicts with (31) and the original conclusion holds. ■

Now we prove our proposition in two steps.

First, we prove that the solution of (29) converges to that of (28). Notice that (28) is a pure two-stage stochastic program, where the first stage decision variables are continuous or discrete and the expectation function in the objective function is continuous. Based on the conclusion in [21], the SAA of this problem converges to the true value of the two-stage stochastic program.

Second, we prove that the solution of (28) converges to that of (27). It is easy to see that our model satisfies all conditions in the above corollary. Then, accordingly, the solution of (28) converges to that of (27).

Therefore, the solution of our SAA problem (29) converges to that of the true problem (27). The conclusion holds.

REFERENCES

[1] R. Barth, H. Brand, P. Meibom, and C. Weber, "A stochastic unit-commitment model for the evaluation of the impacts of integration of large amounts of intermittent wind power," *International Conference on Probabilistic Methods Applied to Power Systems*, pp. 1–8, 2006.

[2] A. Tuohy, P. Meibom, E. Denny, and M. O'Malley, "Unit commitment for systems with significant wind penetration," *IEEE Transactions on Power Systems*, vol. 24, pp. 592–601, 2009.

[3] A. Tuohy, E. Denny, and M. O'Malley, "Rolling unit commitment for systems with significant installed wind capacity," *2007 IEEE Lausanne Power Tech*, pp. 1380–1385, 2007.

[4] B. C. Ummels, M. Gibescu, E. Pelgrum, W. L. Kling, and A. J. Brand, "Impacts of wind power on thermal generation unit commitment and dispatch," *IEEE Transactions on Energy Conversion*, vol. 22, no. 1, pp. 44–51, 2007.

[5] F. Bouffard and F. D. Galiana, "Stochastic security for operations planning with significant wind power generation," in *Power and Energy Society General Meeting - Conversion and Delivery of Electrical Energy in the 21st Century*, Pittsburgh, PA, 2008.

[6] P. A. Ruiz, C. R. Philbrick, E. Zak, K. W. Cheung, and P. W. Sauer, "Uncertainty management in the unit commitment problem," *IEEE Transactions on Power Systems*, vol. 24, pp. 642–651, 2009.

[7] P. A. Ruiz, C. R. Philbrick, and P. W. Sauer, "Wind power day-ahead uncertainty management through stochastic unit commitment policies," in *Proceedings of the IEEE PES Power Systems Conference and Exposition*, Seattle, Wash., 2009.

[8] J. Wang, M. Shahidehpour, and Z. Li, "Security-constrained unit commitment with volatile wind power generation," *IEEE Transactions on Power Systems*, vol. 23, no. 3, pp. 1319 – 1327, 2008.

[9] J. Wang, A. Botterud, V. Miranda, C. Monteiro, and G. Sheble, "Impact of wind power forecasting on unit commitment and dispatch," in *8th Int. Workshop on Large-Scale Integration of Wind Power into Power Systems, Bremen, Germany*, Oct. 2009.

[10] S. Fink, C. Mudd, K. Porter, and B. Morgenstern, "Wind power curtailment case studies," in *National Renewable Energy Laboratory Report. Available at http://www.nrel.gov/docs/fy10osti/46716.pdf*, 2009.

[11] V. Miranda and P. S. Hang, "Economic dispatch model with fuzzy wind constraints and attitudes of dispatchers," *IEEE Transactions on Power Systems*, vol. 20, no. 4, pp. 2143 – 2145, 2005.

[12] A. Botterud, J. Wang, C. Monteiro, and V. Miranda, "Wind power forecasting and electricity market operations," in *The 32nd IAEE International Conference*, San Francisco, California, Jun. 2009.

[13] U. A. Ozturk, M. Mazumdar, and B. A. Norman, "A solution to the stochastic unit commitment problem using chance constrained programming," *IEEE Transactions on Power Systems*, vol. 19, no. 3, pp. 1589 – 1598, 2004.

[14] H. Yu, C. Y. Chung, K. P. Wong, and J. H. Zhang, "A chance constrained transmission network expansion planning method with consideration of load and wind farm uncertainties," *IEEE Transactions on Power Systems*, vol. 24, no. 3, pp. 1568–1576, 2009.

[15] S. Ahmed and A. Shapiro, "Solving chance-constrained stochastic programs via sampling and integer programming," *2008 Tutorials in Operations Research: State-of-the-Art Decision-Making Tools in the Information-Intensive Age*, 2008.

[16] B. K. Pagnoncelli, S. Ahmed, and A. Shapiro, "Sample average approximation method for chance constrained programming: theory and applications," *Journal of Optimization Theory and Applications*, vol. 142, no. 2, pp. 399–416, 2009.

[17] J. R. Birge and F. Louveaux, *Introduction to Stochastic Programming*. Springer Verlag, 1997.

[18] S. J. Wang, S. M. Shahidehpour, D. S. Kirschen, S. Mokhtari, and G. D. Irisarri, "Short-term generation scheduling with transmission and environmental constraints using an augmented Lagrangian relaxation," *IEEE Transactions on Power Systems*, vol. 10, no. 3, pp. 1294–1301, 1995.

[19] J. Luedtke, S. Ahmed, and G. Nemhauser, "An integer programming approach for linear programs with probabilistic constraints," *Mathematical Programming*, vol. 122, no. 2, pp. 247–272, 2010.

[20] A. J. Kleywegt, A. Shapiro, and T. Homem-de Mello, "The sample average approximation method for stochastic discrete optimization," *SIAM Journal on Optimization*, vol. 12, no. 2, pp. 479–502, 2002.

[21] S. Ahmed and A. Shapiro, "The sample average approximation method for stochastic programs with integer recourse," ISyE, Georgia Institute of Technology, GA, Tech. Rep., 2002.

[22] Y. Guan, S. Ahmed, and G. L. Nemhauser, "Sequential pairing of mixed integer inequalities," *Discrete Optimization*, vol. 4, no. 1, pp. 21–39, 2007.

[23] H. Triebel, *Interpolation Theory, Function Spaces, Differential Operators*. North-Holland Amsterdam, 1978.